Journal of Visualization, Vol. 3, No. 4 (2001) 313-321

Preprocessed Visualization of Large Scale Unsteady Flow Simulations

Teramoto, S.*[1] and Fujii, K.*[2]

*1 Department of Aeronautics and Astronautics, School of Engineering, the University of Tokyo, 7-3-1 Hongo, Tokyo 113-8656, Japan.
*2 The Institute of Space and Astronautical Science, 3-1-1 Yoshinodai, Sagamihara, Kanagawa 229-8510, Japan.

Received 7 December 2000.
Revised 5 January 2001.

***Abstract*:** In some cases, conventional CFD visualization techniques do not give us sufficient information of the flowfield, especially when the flowfield is unsteady, and there is a need for a new post-processing technique. In the present paper, one of such new post-processing techniques is proposed. In the present technique, raw result of CFD simulation is pre-processed by frequency filters, and then processed secondary data set is visualized. The idea is applied to two examples. The examples show that the present method visualizes each frequency mode separately, and gives clear view of the temporal variation of the whole flowfield. The results indicate that the present method improves the understandings of the flow mechanism.

***Keywords*:** unsteady flowfields, postprocessing, CFD, large-scale flow structure, shear layer.

1. Introduction

Nowadays, Computational Fluid Dynamics (CFD) is applied to many engineering problems. Total number of grid points used in practical simulations can easily reach millions to tens of millions, and the advances in computing technologies allow us to carry out such large-scale simulations within reasonable turn-around time.

It has been pointed out that the pre-processing stage of such large-scale simulations occupies large part of the total analysis time. At the same time, the time required for the post-processing increases as the simulation becomes sophisticated, especially when the flowfield is unsteady. The typical size of the flowfield data with ten million grid points is 400 MB, and hundreds of such data sets are required to resolve temporal characteristics of unsteady phenomena. In other words, hundreds giga-bytes data have to be manipulated in the post-processing. Handling of the data files requires difficult and time-consuming work.

Such flowfield data includes spatial variations such as shock waves, vortices, shear layers and else, and these spatial features move in time. It is often the case that we are interested in only a part of these features, but it is difficult to distinguish separate characteristic feature in interest, since all the features are overlaid in the raw data obtained from the simulation.

Several methods have been developed for the efficient detection of spatial features, such as vortex core (Sawada, 1995; Haimes and Kenwright, 1999), shock wave (Lovely, 1999) and separation and reattachment (Kao and Shen,1999), out of the simulation data. These methods give clearer view of the spatial structure of the flowfields, and they help our understanding of the flowfield. However, they do not reduce the temporal complexity of the flowfields. In most cases, temporal variation of the flowfield is discussed only by the animations created from raw results of the simulation, and there seems to be little effort for the development of a method that detects temporal characteristics from time series of the flow variables.

With increasing temporal complexities of the CFD problems, visualization techniques that detect temporal characteristics of the flowfield are becoming important in the post-processing of unsteady flow simulations. In the present paper, a simple but useful filtering technique is proposed for the better understanding of the temporal characteristics of the flowfield.

2. Visualization of Unsteady Flowfield

One of the important objectives of the post-processing is to help understanding the flowfield, and the first step of the post-processing is the identification of the characteristic features.

Visualization is one of the useful methods of post-processing of steady flow simulations. The visualization provides us intuitive view of the spatial features, and helps our understanding of the mechanism of the flowfield. Figure 1 is an example of the visualized images. It shows the transonic flowfield around a reentry capsule. The free-stream Mach number is 1.3, and the pitch angle is 10°. The shade of the background denotes the density gradient distributions, the color of the capsule surface shows the surface pressure distributions, and the streamlines are visualized as blue lines in the figure. Key spatial features, such as the locations of shock waves, wake, surface pressure distributions and streamlines behind the capsule, are all displayed in the figure. One can easily recognize the static mechanism of the flowfield from this figure: for example, the flow separates at the edge of the capsule, the recompression shock wave emanates from the neck of the wake and large-scale vortices exist inside the recirculation region behind the capsule.

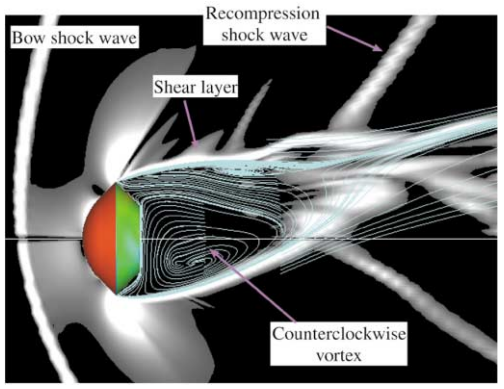

Fig. 1. Transonic flowfield around a reentry capsule.

On the other hand, simple visualization does not necessarily provide sufficient information about the mechanism of the flowfield especially when the flowfield is unsteady. Figures 2(a)-(c) show the flowfield behind the capsule oscillating in pitch (Teramoto and Fujii, 2000). The geometry of the capsule and the flow conditions are the same as those in Fig. 1. The free stream Mach number is 1.3, the diameter of the capsule is 0.1 m, the capsule is oscillating in pitch at 20 Hz and the resultant non-dimensional frequency is about 0.03. The capsule is pitching down from $\alpha = +5.8^{\circ}$ to $\alpha = -13.1^{\circ}$ in the figures, where α denotes the angle of attack. In Figs. 2(a)-(c), marker particles are released behind the capsule in a line at certain intervals. Each particle line is colored by different colors.

The large-scale vortices shown in Fig. 1 are the key features of the flowfield (Teramoto and Fujii, 1999), and therefore the correlation between the attitude of the capsule and the vortices is a point of interest in the discussion. The motion of the vortices is expected to be visualized by the deformation of the particle lines. However, the particles are scattered soon after the release, and it is difficult to identify large-scale vortices from the figures. The power-spectrum density diagram (Fig. 3) shows that the fluctuation of the base pressure has a high-frequency component near 1 kHz, in addition to the low-frequency harmonic components induced by the motion of the capsule. These high-frequency fluctuations scatter the marker particles, and conceal the slow motion of the large-scale vortices.

These two examples show that the visualization is an effective method for the identification of spatial features, but in some cases, simple visualization is not sufficient to identify temporal features.

In such cases, we usually select several representative locations, extract time history of the data at these

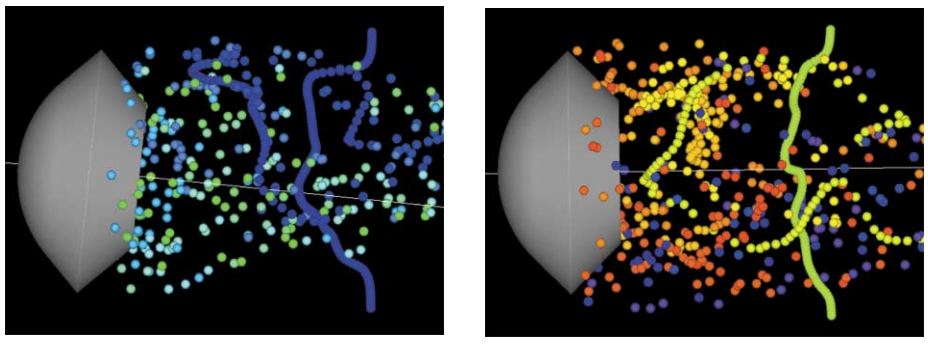

(a) a = 5.8° (pitching down)

(b) a = –0.8° (pitching down)

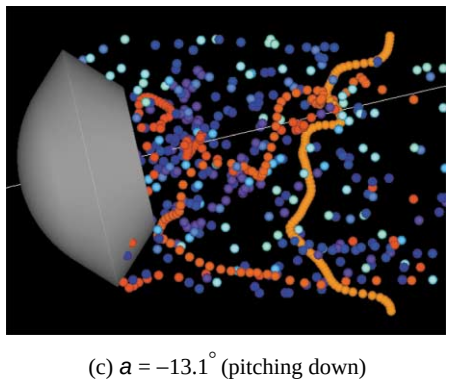

(c) a = –13.1° (pitching down)

Fig. 2. Particle traces behind the oscillating capsule (Raw data).

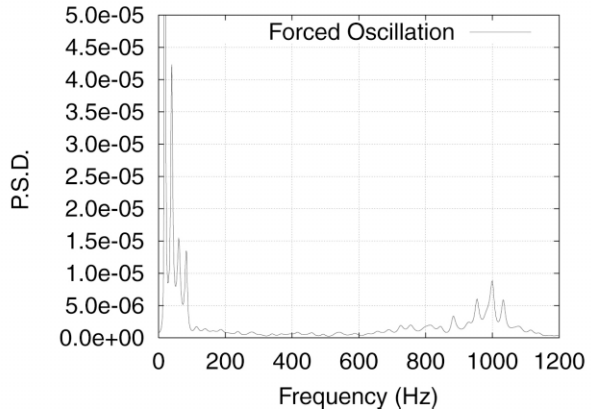

Fig. 3. Power spectrum density of the base pressure.

points, analyze temporal characteristics of the flow variables for instance, by the spectrum analysis, and then discuss the behavior of the whole flowfield. It is not easy, however, to discuss the whole flowfield only from the several pointwise information. Large amount of data obtained in the simulation is not efficiently used in this approach.

3. Proposed Method

3.1 Pre-processed Visualization

Since it is difficult to identify temporal features directly from the visualized images, it may be useful to pre-process the simulation result and visualize the reconstructed secondary data. If the temporal features are successfully extracted by the pre-processing, temporal behavior of the spatial features may be easily observed.

There are many ways to extract temporal features from the raw data, and as a first step, time histories of the flow variables are pre-processed by frequency filters and visualized as follows:

1. take the time history of the typical flow variable at the point representing the flowfield,
2. decompose the history into frequency modes using Fourier analysis,
3. select the mode to visualize,
4. define the frequency range of the frequency filter, pre-process the time history of the flow variables at all the points by the frequency filter to eliminate other frequency components, and create time history of the secondary data set of the whole flowfield,
5. visualize the created data set of the filtered flow variables,
6. create animation.

Note that the size of the data set after the filtering is the same as the original data set, and the steps (5) and (6) are the same processes as those used in the conventional post-processing of unsteady flow simulations. However, the temporal complexity has already been reduced by the filtering, and the filtered data may provide clearer view of the temporal features of the flowfield.

3.2 Digital Filter

Numerical simulations using millions of nodes output tens to hundreds MB data file, and *n*-th order digital filter requires *n* data sets to be stored on the main memory during the execution process. On the other hand, the main memory size of the modern workstation is hundreds MB to several GB. Higher order digital filter gives sharper cut-off characteristic in general, but allowable order of the filter is at most ten, due to the limitation of the memory.

There are two types of digital filters (Kuc, 1982), FIR (Finite Impulse Response) filter and IIR (Infinite Impulse Response) filter. FIR filter is simple and robust, but it requires 10th or higher order to obtain practical cut-off characteristics. IIR filter gives sharp cut-off characteristic with lower order, but high-order single stage IIR filter tends to be numerically unstable. Therefore, second-order IIR filter connected in series is used in the present study, to obtain both the sharp cut-off characteristics and the numerical stability.

Figure 4 shows the characteristics of the 4th order Butterworth low-pass filter as an example of the IIR digital filter. The cut-off frequency f_c is 1000 Hz. The filter causes 0.4 msec of delay at the low frequency region, and therefore the delay has to be compensated when comparing the filtered value with the non-filtered one. The delay also shows slight overshoot near the cut-off frequency 1 kHz. The cut-off frequency has to be carefully selected so that it is kept far away from the dominant frequencies of the phenomena. Otherwise, the filtering process distorts the flowfield and may output misleading results.

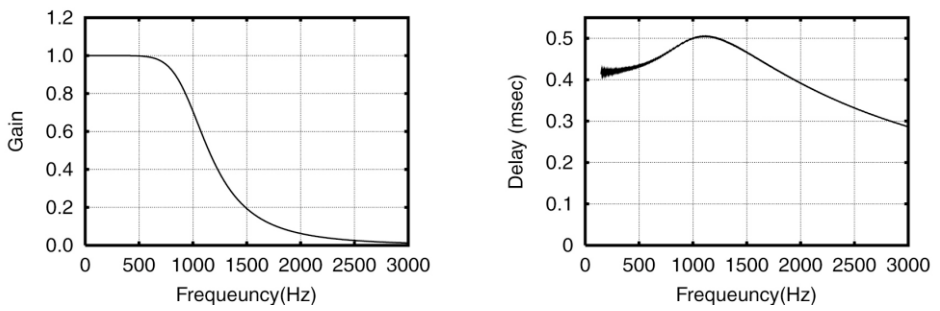

(a) Gain (b) Delay

Fig. 4. Characteristics of Butterworth LPF (n = 4, f_c = 1000 Hz).

4. Numerical Examples

4.1 Vortex Structure behind a Capsule in the Pitching Oscillation

The proposed pre-processing technique is first applied to the flowfield shown in Fig. 2. Time series of the physical properties are pre-processed by the low-pass filter (LPF) which has the cut-off frequency at 150 Hz, and the result is visualized in Figs. 5(a)-(d). The particle traces show the velocity field behind the capsule and the color of the

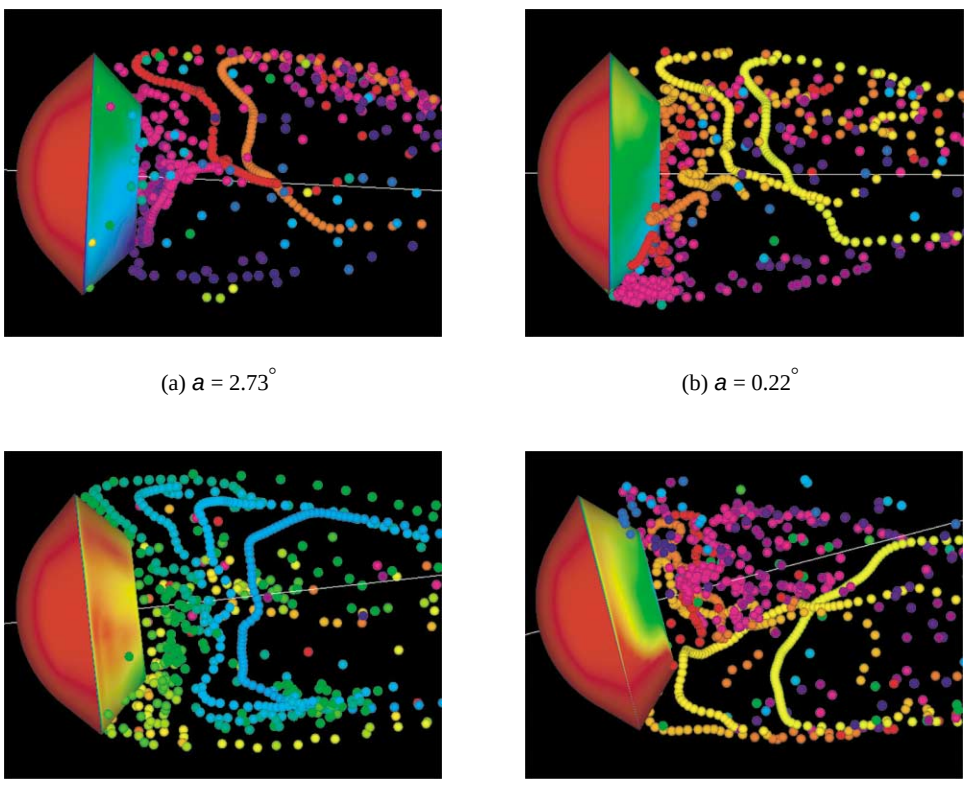

Fig. 5. Particle traces behind the oscillating capsule (Filtered data).

capsule surface shows the surface pressure distributions. All the flow conditions are the same as those of Fig. 2, and the marker particles are released from the same position at the same interval as used in Fig. 2.

High frequency disturbances near 1 kHz (Fig. 3) that scattered the marker particles in Fig. 2 are suppressed by the filtering, and the dynamic behavior of the flowfield becomes clear in Fig. 5. When the pitch angle is positive (Fig. 5(a)), a large counterclockwise vortex can be recognized in the lower region. At the moment of Fig. 5(b), the pitch angle of the capsule is almost zero, but the counterclockwise vortex is still dominant behind the capsule and the surface pressure is higher at the upper side of the base than that at the lower half. As the capsule further pitches down, the counterclockwise vortex gradually diminishes (Fig. 5(c)) and a small clockwise vortex is formed at the upper side. It gradually develops and propagates upstream, and finally becomes a clear clockwise vortex at the upper side (Fig. 5(d)). These figures also show that the base pressure distributions are related to the vortex structure behind the capsule. The surface pressure at the upper side of the base is higher than that of the lower half when the counter clockwise vortex is dominant behind the capsule (Figs. 5(a)-(c)). The surface pressure at the lower part does not exceed that at the upper part until the clockwise vortex becomes dominant behind the capsule (Fig. 5(d)).

The present filtering technique improved *S/N* ratio of the visualized images. The motion of the large-scale vortices as well as the correlation between the vortices and the base pressure distributions are clearly observed from the pre-processed image.

4.2 Oscillation of the Shear Layer in the Supersonic Cavity Flow

Second example is a supersonic flow over a cavity. The flowfield around the cavity has been well studied, and it is well known that the pressure fluctuation in the cavity shows several harmonic tones (Rossiter, 1966; Rizzetta, 1988).

The numerical simulation is carried out with the upstream Mach number 1.83. A cavity is attached to the

lower wall of the 60mm × 60mm square duct. The depth of the cavity is 20mm, the width and the length are both 60 mm (Fig. 6).

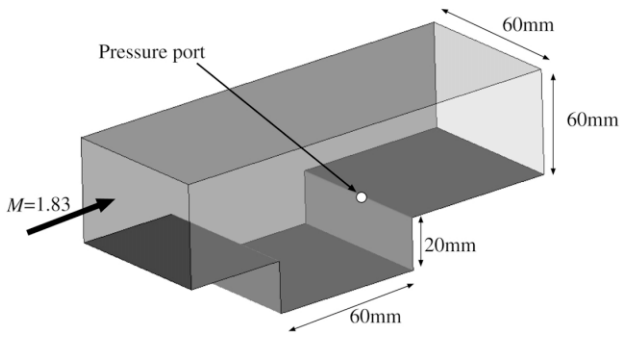

Fig. 6. Supersonic cavity.

Figure 7 shows the power-spectrum density of the pressure fluctuation at the middle of the upper edge of the rear cavity wall. A sharp tone is observed at 4.6 kHz, and its bi- and tri-harmonic tones appear at 9.15 kHz and 13.5 kHz. More smooth peaks are also observed at 2.2 kHz, 6.4 kHz and so on. Each tone corresponds to its own exciting mechanism, and the shear layer oscillates with the particular pattern which is related to the flow mechanism at each frequency. The dynamic behavior of the flowfield inside the cavity is not fully understood, and there are still discussions about the mechanism of the excitation.

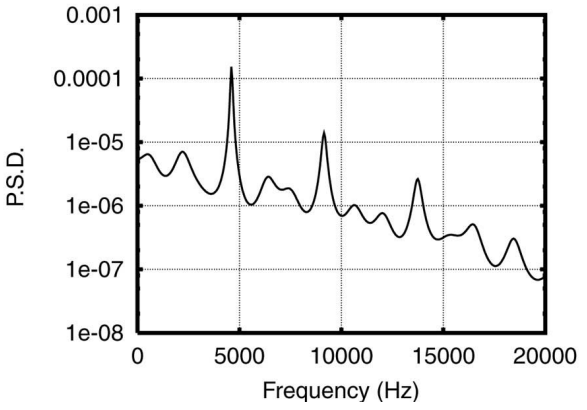

Fig. 7. Power spectrum density of the rear wall pressure.

The shear layer is visualized as the iso *y*-vorticity surface in Figs. 8(a)-(d). These figures show that the disturbance of the shear layer propagates both streamwise and spanwise. However, the amplitude of the oscillation of the shear layer is so small, and the oscillation is the superposition of several fundamental oscillation patterns. Therefore, it is almost impossible to identify the meaning of each frequency. Here, time series of the physical properties are pre-processed by the band-pass filter (BPF) and the oscillation pattern corresponding to each harmonic tone is visualized separately.

Figure 9(a) shows the iso surface of the streamwise *x*-momentum contours filtered by the BPF of 3.5 kHz-5.5 kHz. The frequency range corresponds to the most prevailing harmonic tone. As the streamwise momentum at the upper side of the shear layer is larger than that at the lower side, the fluctuation of the streamwise momentum is negative (colored blue) where the shear layer shifts upward, and it is positive (colored orange) where the shear layer shifts downward. Both the blue regions and the orange regions spread full-span and they appear streamwise alternatively. The streamwise length of each region is about half of the cavity length. These patterns show that the most prevailing mode at 4.6 kHz is the two-dimensional flapping mode, and its wavelength is equal to the length of the cavity.

The oscillation of the shear layer that corresponds to the lower harmonic tone (2.2 kHz) shows different

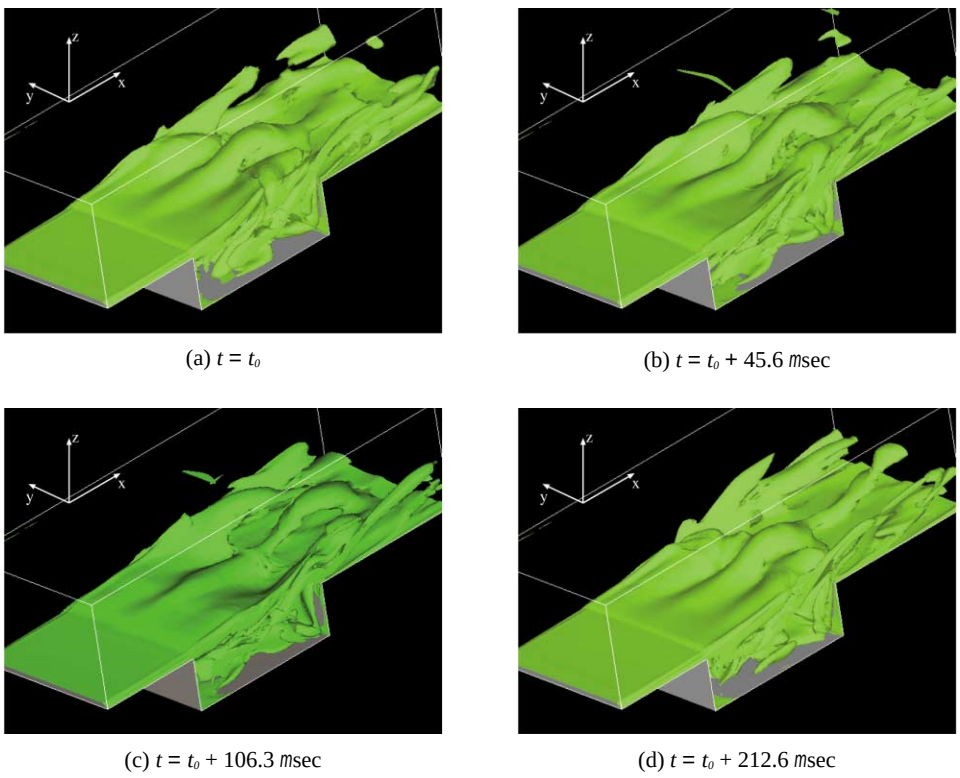

(a) $t = t_0$ (b) $t = t_0 + 45.6$ msec

(c) $t = t_0 + 106.3$ msec (d) $t = t_0 + 212.6$ msec

Fig. 8. Fluctuation of the shear layer (Raw data, iso *y*-vorticity surface).

pattern. Iso surfaces of the streamwise momentum contours pre-processed by the BPF of 1.5 kHz - 3 kHz are shown in Fig. 9(b). The positive region is colored yellow-green, and the negative region is colored blue-green in this figure. Each contour surface spreads streamwise, and the yellow-green regions (shear layer shifts downward) and the blue-green regions (shear layer shifts upward) appear side by side. These patterns indicate that the shear layer is disturbed by the intermittent shedding of the longitudinal vortices.

The present filtering method emphasizes the motion of the shear layer, and visualizes the difference in the fluctuation of the shear layer at each frequency. It would be difficult to recognize these differences from the pointwise information obtained by the conventional approach.

5. Discussions

The technique that pre-processes original raw data is not a new idea. It is widely used in the post-processing of experimental data or in the pointwise analysis of the result of numerical simulations. Key concept of the present approach is the combination of the pre-processing and the visualization.

The pointwise analysis utilizes pre-processing alone. This method is useful to identify temporal features, but it is not useful to identify spatial features. In the conventional post-processing using simple visualization of the original raw-data, all the spatial and the temporal features appear in the animation, but it is not easy to distinguish many features, especially when several temporal features (i.e. several oscillations at different frequencies) are overlaid.

The pre-processing is suitable for the discussion of temporal features, and the visualization is suitable for the discussion of spatial features. In the present method, time histories of physical properties at all the points are pre-processed by the frequency filter. The reconstructed secondary data set contains only one or few temporal features, and therefore, we can observe the “spatial distributions of the temporal feature” by the visualization.

The validity of the frequency filter is based on the assumption that the fluctuation of the flowfield can be linearly decomposed into individual mode. Unfortunately, the governing equations of fluid are non-linear, and the above assumption is not self-evident. The fluctuations for the different modes may influence each other, and the filtering might derive misleading results in some cases, especially when the frequencies are close to each other.

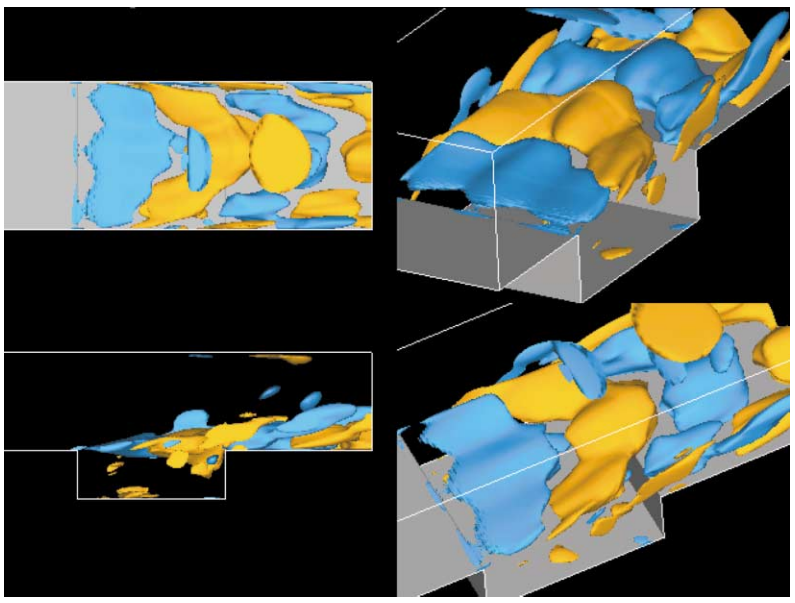

(a) Oscillation at 4.6 kHz (Filtered by BPF (3.5 kHz-5.5 kHz))

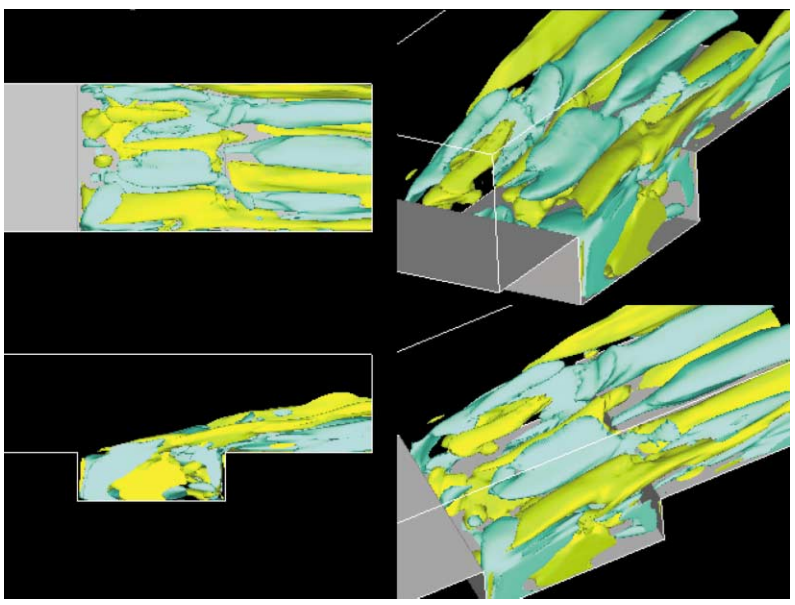

(b) Oscillation at 2.2 kHz (Filtered by BPF (1.5 kHz-3 kHz))

Fig. 9. Fluctuation of the shear layer (Filtered data, iso *x*-momentum surface).

Therefore, the present filtering technique should be complementally used with the conventional post-processing such as the raw data animation and pointwise analysis. Nevertheless, the present idea gives intuitive view of the temporal variation of the whole flowfield, which is never expected by the conventional methods, and this new idea would be a useful technique for the discussion of the results of unsteady flow simulations.

6. Conclusion

The pre-processed visualization method was proposed as a new post-processing technique of unsteady flow simulations. In the present method, time histories of the raw physical properties at all the grid points are pre-processed by frequency filters before the visualization. Complicated oscillation of the flowfield is decomposed into individual mode by the pre-processing. The reconstructed secondary data for each mode is visualized one by one, and the mechanism of each mode is discussed separately. The idea was applied to two examples of unsteady flow

simulations. Both examples showed that the proposed filtering technique successfully visualized the temporal features of the flowfield, and improved the understanding of the flow mechanism.

The present method should be used complementally with the conventional post-processing technique, as it might derive misleading result due to the non-linearity of the fluid flows.

References

Haimes, R. and Kenwright, D., On the Velocity Gradient Tensor and Fluid Feature Extraction, AIAA Paper 99-3288, (1999-6).

Kao, D. L. and Shen, H., Automatic Surface Flow Feature Visualization, AIAA Paper 99-3287, (1999-6) .

Kuc, R., Introduction to Digital Signal Processing, (1982), McGraw-Hill, New York.

Lovely, D., Shock Detection from Computational Fluid Dynamics Results, AIAA Paper 99-3285, (1999-6).

Sawada, K., A Convenient Visualization Method for Identifying Vortex Cores, Trans. Japan Soc. Aero. Space Sci., 38-120 (1995), 102-120.

Teramoto, S. and Fujii, K., Computational Study of the Flow Field behind Blunt Capsules at Transonic Speeds, AIAA Paper 99-3414, (1999-6).

Teramoto, S. and Fujii, K., Study on the Mechanism of the Instability of a Re-entry Capsule at Transonic Speeds, AIAA Paper 2000-2603, (2000-6) .

Rizzetta, D. P., Numerical Simulation of Supersonic Flow Over a Three-Dimensional Cavity, AIAA Journal, 26-7, (1988-7).

Rossiter, J. E., Wind-Tunnel Experiments on the Flow over Rectangular Cavities at Subsonic and Transonic Speeds, Aeronautical Research Council RM 3438, (1966).

Author Profile

Susumu Teramoto: He received his BS Degree in 1992 and his MS Degree in 1994 from the University of Tokyo. After the graduation, he worked for Ishikawajima-Harima Heavy Industries at Research & Development division, and took part in the development of supersonic propulsion system. He moved to the Institute of Space and Astronautical Science (ISAS) in 1997, and obtained his Ph.D in Engineering from the University of Tokyo in 2000. He is currently a Lecturer at the University of Tokyo. His current research involves CFD analysis of high-speed flows related to space launching systems.

Kozo Fujii: He received his Ph.D. in the Department of Aeronautics, University of Tokyo in 1980. After spending two years at NASA Ames Research Center as a NRC research associate, he became a researcher at the National Aerospace Laboratory (NAL) in Japan. After spending a few years again at NASA Ames Research Center as a senior NRC research associate during his research period at the NAL, he joined the Institute of Space and Astronautical Science as an associate professor in 1988. Currently, he is a professor of the high-speed aerodynamics division. He has been engaged in the computational fluid dynamics research. The research area spreads all the aspects of computational fluid dynamics; grid generation, simulation algorithms, flow visualization as well as the applications.